Cooper, A.K., O'Brien, P.E., and Richter, C. (Eds.)
Proceedings of the Ocean Drilling Program, Scientific Results Volume 188

10. Synthetic Seismograms Linking ODP Sites to Seismic Profiles, Continental Rise and Shelf of Prydz Bay, Antarctica[1]

D.A. Handwerger,[2] A.K. Cooper[3], P.E. O'Brien,[4] T. Williams,[5] S.R. Barr,[6] R.B. Dunbar,[3] A. Leventer,[7] and R.D. Jarrard[2]

ABSTRACT

Synthetic seismograms provide a crucial link between lithologic variations within a drill hole and reflectors on seismic profiles crossing the site. In essence, they provide a ground-truth for the interpretation of seismic data. Using a combination of core and logging data, we created synthetic seismograms for Ocean Drilling Program Sites 1165 and 1166, drilled during Leg 188, and Site 742, drilled during Leg 119, all in Prydz Bay, Antarctica. Results from Site 1165 suggest that coring penetrated a target reflector initially thought to represent the onset of drift sedimentation, but the lithologic change across the boundary does not show a change from predrift to drift sediments. The origin of a shallow reflector packet in the seismic line across Site 1166 and a line connecting Sites 1166 and 742 was resolved into its constituent sources, as this reflector occurs in a region of large-scale, narrowly spaced impedance changes. Furthermore, Site 1166 was situated in a fluvio-deltaic system with widely variable geology, and bed thickness changes were estimated between the site and both seismic lines.

INTRODUCTION

Synthetic seismograms are useful tools for linking drill hole geology to seismic sections in the deep sea because they can provide a direct

[1]Handwerger, D.A., Cooper, A.K., O'Brien, P.E., Williams, T., Barr, S.R., Dunbar, R.B., Leventer, A., and Jarrard, R.D., 2004. Synthetic seismograms linking ODP sites to seismic profiles, continental rise and shelf of Prydz Bay, Antarctica. *In* Cooper, A.K., O'Brien, P.E., and Richter, C. (Eds.), *Proc. ODP, Sci. Results,* 188, 1–28 [Online]. Available from World Wide Web: <http://www-odp.tamu.edu/publications/VOLUME/CHAPTERS/010.PDF>. [Cited YYYY-MM-DD]
[2]Department of Geology and Geophysics, University of Utah, 135 South 1460 East, Room 719, Salt Lake City UT 84112, USA. Correspondence author: **akcooper@pangea.stanford.edu**
[3]Department of Geological and Environmental Sciences, Stanford University, Building 320, Room 118, Palo Alto CA 94305, USA.
[4]Petroleum and Marine Division, Australian Geological Survey Organisation, GPO Box 378, Canberra ACT 2601, Australia.
[5]Borehole Research Group, Lamont-Doherty Earth Observatory of Columbia University, Route 9W, PO Box 1000, Palisades NY 10964, USA.
[6]Leicester University Borehole Research, Department of Geology, University of Leicester, University Road, Leicester LE1-7RH, United Kingdom.
[7]Department of Geology, Colgate University, 13 Oak Drive, Hamilton NY 13346, USA.

Initial receipt: 23 July 2002
Acceptance: 15 August 2003
Web publication: 11 February2004
Ms 188SR-010

link between observed marine lithologies and seismic reflection patterns. Reflection profiles are sensitive to changes in sediment impedance, the product of compressional wave velocity and density. Changes in these two physical parameters do not always correspond to observed changes in lithologies. By creating a synthetic seismogram based on sediment petrophysics, it is possible to identify the origin of seismic reflectors and trace them laterally along the seismic line.

Ocean Drilling Program (ODP) Leg 119 scientists generated synthetic seismograms for Sites 739 and 742 in Prydz Bay (Shipboard Scientific Party, 1989b), ~40 km northeast of Site 1166 from Leg 188. We created synthetic seismograms using downhole logging- and core-based physical properties data for Sites 742, 1165, and 1166. The synthetic seismogram for Site 1165 is linked to a seismic profile collected during Leg 188. Site 1166 is linked to two seismic profiles (Fig. **F1**). The first was collected during a 1982 expedition to Prydz Bay by the Australian Bureau of Mineral Resources (now AGSO, the Australian Geological Survey Organization). The second profile was collected in February 2001 by the *Palmer* to join Sites 1166 and 742, so we provided a new synthetic seismogram for Site 742 for comparison with the *Palmer* line. The original Site 742 synthetic seismogram, created shipboard during Leg 119, was linked to a profile gathered during the cruise (Shipboard Scientific Party, 1989b) and is not reproduced here.

Drilling at Site 1165 was undertaken to obtain a complete Miocene to Holocene high-resolution section of the Wild Drift, on the continental rise of Prydz Bay (Fig. **F1**). Regional reflector P3 (Fig **F2;** Shipboard Scientific Party, 2001a) was chosen as the target depth of drilling. Reflector P3, which is the same as reflector P2 of Kuvaas and Leitchenkov (1992), was thought to represent the onset of drift sedimentation, possibly related to the initiation of the Antarctic Circumpolar Current after the opening of the Drake Passage at the Oligocene/Miocene boundary (Kuvaas and Leitchenkov, 1992; Shipboard Scientific Party, 2001a). One of the motivations for creating the synthetic seismogram for this site was to evaluate whether coring indeed crossed reflector P3. If reflector P3 was crossed, then it remained to be determined whether it represents the onset of drift sedimentation. To answer this question, the exact location of the petrophysical change that led to the reflector needs to be known, to see if it corresponds to an observed lithologic change from predrift to drift sedimentation.

One objective for generating the synthetic seismogram at Site 1166 was identification and separation of the contributions of several large but closely spaced lithologic changes to a major reflector package in the seismic profile (Fig. **F3**). Furthermore, a section that spans the initial arrival of glacial ice at the continental margin was recovered at Site 1166, and a synthetic seismogram should be able to identify the reflector in the section associated with this event, if one exists.

A section was recovered at Site 742 that was similar to the upper portion of Site 1166, including some of the large, closely spaced impedance contrasts that confuse the reflector pattern at Site 1166. Identification of the contributions of these impedance contrasts at Site 742 to overall reflector patterns in the seismic profile should allow for similar seismic features at both sites to be traced across the *Palmer* line (Fig. **F3B**).

F1. Location map for ODP sites and AGSO and *Palmer* seismic lines, p. 14.

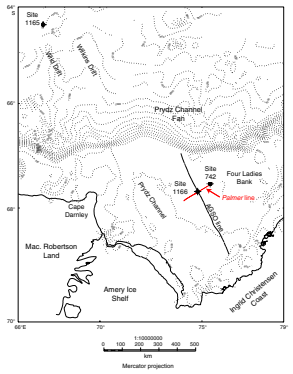

F2. Seismic section, Site 1165, p. 15.

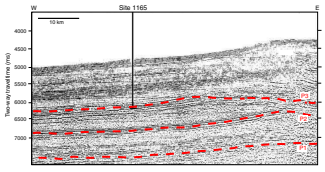

F3. Seismic section, Site 1166, p. 16.

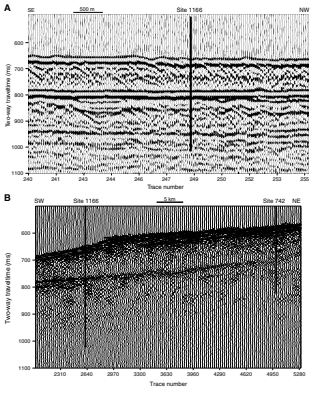

DATA SETS

Sites

Site 1165 was drilled into the Wild Drift, on the continental rise of Prydz Bay, at a water depth of ~3500 m (Fig. F1). Approximately 1 km of predominantly diatom clay to thinly bedded claystone of early Miocene to Holocene age was collected over two main holes (1165B and 1165C). Hole 1165C was started as the result of a change in bottom-hole assembly and switch to rotary core barrel (RCB) drilling. Total recovery for Site 1165 was ~69%, with higher recovery in Hole 1165C than Hole 1165B. Hole 1165A consisted of a single mudline core. Because of hole stability concerns, Hole 1165C was logged from ~980 to ~175 meters below seafloor (mbsf). The drill pipe had to be held at ~175 mbsf to prevent hole collapse, and no density or sonic logs can be collected through the pipe steel.

Site 1166 was drilled into the southwest flank of the Four Ladies Bank, on the Prydz Bay continental shelf, in ~475 m of water (Fig. F1). Coring likely penetrated a fluvial system with buried relief, and Site 1166 drilled into a buried high-standing area (e.g., channel bank) that deepens sharply to the northeast (**Erohina et al.,** this volume; Fig. F3). The upper part of the lithologic section consisted of a thick glacial diamict unit of Pliocene to Holocene age with one interbed of Pliocene sandy/clayey silt. Underlying this is a 21-m-thick late Eocene to early Oligocene proglacial claystone with sandy layers and clasts. Below ~170 mbsf is ~200 m of homogeneous late Eocene coarse-sand fluvial/deltaic sediments overlying Cretaceous clays. The basal portion of the coarse sands shows soft-sediment deformation and contains black organic-rich material. The two dominant lithologies, diamict and coarse sand, are both difficult to collect in marine cores, so overall recovery for this site was only ~18%.

Approximately 40 km northeast of Site 1166, on the eastern portion of Four Ladies Bank, Site 742 was cored during Leg 119 in ~415 m of water (Fig. F1). Site 742 is dominated by diamict sediments from the base of the section in the Oligocene–Eocene to the top in the Quaternary. Variations in the diamict include homogeneous diamictite from the late Pliocene to Quaternary, a thin stratified diamict in the early to late Pliocene, and calcareous diamictite in the Eocene–Oligocene, which makes up about half of the section. Recovery at Site 742 was ~53%. The thick, homogeneous sands that contributed to the poor recovery at Site 1166 were not recovered at Site 742. The lowermost 2 m of Site 742, however, did yield a lithology similar to the deformed sands with organic material recovered at Site 1166.

Seismic Reflection Surveys Used

A single-channel reflection profile across Site 1165 was collected aboard the *JOIDES Resolution* during a presite survey upon arrival at the site. The seismic source was an 80-in^3 (1310 cm^3) water gun, operated at ~1900 psi (13.1 MPa) and towed ~20 m behind the ship. It was fired every 10 s, and with a ship speed of 6.5 kt yielded a shot every ~33 m. Reflections were recorded by a Teledyne model 178 hydrostreamer of 60 hydrophones towed at ~12–18 m depth. Depth-stabilizing "birds" were not available for use on the streamer. Data from each shot were sampled every 4 ms over a 4-s window and digitally recorded in SEG-Y format af-

ter application of a 20- to 250-Hz filter (Shipboard Scientific Party, 2001b). Individual traces were extracted and a five-trace average about the shotpoint nearest the drill site was used for comparison with the synthetic seismogram. Sampling interval was 2000 ms.

Multichannel seismic data for Site 1166 were collected by the Australian Bureau of Mineral Resources (now AGSO) in 1982. The survey was typically recorded sixfold on a Teledyne 178 hydrostreamer, configured in six 50-m active sections. The source was a 460-in^3 (7538 cm^3) bolt air gun. Ship positions were recorded every 10 s using a Tracor Mk 2 satellite navigator (Shipboard Scientific Party, 2001c). Data were filtered from 8 to 200 Hz, and individual stacked traces were extracted for comparison to the synthetic seismogram. Sampling interval was 4000 ms.

The high-resolution single-channel seismic data on *Palmer* line 01-1-4 were acquired by the *Palmer* in February 2001 using a single 90-in^3 (1475 cm^3) generator injector air gun fired every 6 s at a ship's speed of ~5 kt, yielding a distance between shotpoints of ~15 m (A. Cooper, pers. comm., 2002). The data were stored in SEG-Y format and bandpass filtered using a tapered window between 6–10 and 170–230 Hz for display and analysis. The sampling interval was 500 ms.

The AGSO line ran roughly north–south and crossed the midflank of the channel bank Site 1166 was drilled into. The *Palmer* line trended roughly southwest–northeast, with decreasing channel bed thickness at Site 742 relative to Site 1166 (Fig. **F1**).

METHODS

Wavelets

None of the seismic profiles used in this study have directly measured seismic wavelets. Therefore, the seafloor reflector was used in each case to determine the wavelet. Because of the likelihood of shallow reflectors at Sites 1166 and 742, the seafloor reflector was extracted exclusively from shotpoints distant from the drill sites. This was not the case for Site 1165, which was cored in a sediment drift of laterally uniform sedimentation and was therefore unlikely to contain significant local reflectors.

Wavelet for the *JOIDES Resolution* Section (Site 1165)

The source wavelet used for the Site 1165 synthetic seismogram was extracted from an average of the seafloor reflections of two widely spaced traces (shotpoints 1000 and 1191, the latter near the drill site) (Fig. **F4A**). Internal consistency of the wavelet over this substantial distance confirms the reliability of using the seafloor reflection (Fig. **F4A**). Unfortunately, the seismic source was a water gun and so the wavelet is tripeaked, spans a width of ~90 ms, and consists of a ~23-ms precursor. It was resampled to 0.2 ms, the same as the Site 1165 composite impedance log, for convolution.

Wavelet for the AGSO Line (Site 1166)

Seafloor reflections at three widely spaced shotpoints (300, 1102, and 2461) were initially considered for wavelet extraction (Fig. **F4B**). All three shotpoints show two peaks at consistent spacing. However, two of the shotpoints (300 and 2461) show a possible third peak, but at

F4. Wavelets used to create the synthetic seismograms, p. 17.

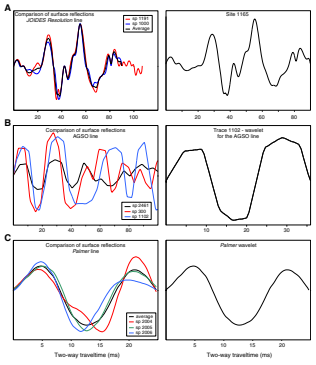

slightly different arrival times and with different shapes. The third shotpoint (1102) does not show this third peak, which could be caused by a shallow reflector, and it was therefore considered to have a character most representative of a simple seafloor reflection. The lithologic section recovered at Site 1166 contained ~2.6 m of hemipelagic sediments overlying diamictite. The contact between these two units may produce the third peak found near the seafloor reflection at the shotpoint nearest the drill site. The wavelet that was used, therefore, consists of two peaks and is ~37 ms long. Including the third peak degraded the match between the synthetic seismogram and seismic section. No low-amplitude precursor was recorded.

Wavelet for the *Palmer* Line (Sites 1166 and 742)

The wavelet for the *Palmer* line was extracted from the average seafloor reflection of shotpoints 2004–2006 (Fig. F4C). The shotpoints nearest both Sites 1166 (shotpoint 2637) and 742 (shotpoint 4999) were very ringy, possibly the result of a shallow reflector occurring at the contact between surficial hemipelagic sediments and underlying diamicts. This is consistent with the inferred shallow reflector based on extraction of the seafloor reflection from the AGSO line as well. The seismic profile gathered during Leg 119 over Site 742 recorded a direct arrival from the water gun aboard the *JOIDES Resolution* and shows a character similar (but of longer duration) to the inferred wavelet for the *Palmer* line (Shipboard Scientific Party, 1989b), whereas the seismic section is ringy in the near surface.

The seafloor reflection at shotpoints 2004–2006 consisted of two peaks and one trough over a duration of ~27 ms. At the drill sites, the seafloor reflections contained five peaks and lasted 50 ms. Synthetic seismograms created with the drill site–based wavelets appeared too ringy throughout, whereas synthetic seismograms created with the wavelet from shotpoints 2004–2006 closely matched the nearby seismic traces.

Creation of the Impedance Logs

Site 1165

Downhole velocity logging was undertaken for only ~40% of Hole 1165, and most of this log was unreliable, characterized by abundant cycle skips (Shipboard Scientific Party, 2001b). As a result, we used a composite velocity log to create the impedance log for Site 1165. This composite was derived primarily from logging density data and from core index velocities above and below the logged interval.

For synthetic seismograms, there are a number of advantages to using logging rather than core data: (1) logs are continuous, whereas core data are limited to recovered intervals; (2) logging data are recorded in situ, whereas cores expand due to pressure release as they are brought to the surface (Hamilton, 1976); and (3) logging data are unaffected by drilling disturbance. Drilling disturbance in cores increases considerably whenever extended core barrel (XCB) or RCB drilling techniques are required. The latter two were used for a majority of coring at Site 1165, with XCB coring used to the base of Hole 1165B and RCB used entirely for Hole 1165C.

The density log for Site 1165 was much longer (175–985 mbsf) and more reliable than the sonic log. Nevertheless, the litho-density tool,

which measures bulk density, requires contact with the borehole wall. Where the borehole is ragged or too wide for good tool contact against the wall, the bulk density data are typically unreliable. In contrast, the resistivity log is relatively insensitive to hole conditions. Both resistivity and bulk density primarily respond to changes in porosity, so comparison of those logs can indicate regions of suspect density data. We subjectively edited the density log to remove spurious intervals, based on comparison to the resistivity, caliper, and bulk density correction factor logs. The edited regions were generally no more than a few meters thick, and linear interpolation was used to span regions of deleted density data. From the seafloor to the top of the density log at 175 mbsf and from the bottom of the density log to the total depth of the hole (985–999 mbsf), index velocities were used. Vertical core velocities were typically used since this direction is more representative of the formation as seen by vertically penetrating seismic waves. From 94 to 175 mbsf, however, vertical velocities were not recorded, so horizontal velocities were used. The moisture and density–derived (index) densities above the log were corrected to in situ conditions (Fig. **F5A**) based on comparison between the index and logging densities within the logged interval.

Where index velocities were used, the values had to be converted to in situ conditions, as cores rebound when exposed to atmospheric pressure (Hamilton, 1976, 1979). This correction was based on comparison of logging velocity to index velocity in the several intervals for which sonic logging data were reliable. Reliability of the velocity log was determined based on character match of the *P*-wave velocity log to the more robust resistivity log, in a manner similar to the comparison made between the resistivity and density logs. As sonic velocity is also primarily responsive to changes in porosity in the marine system, the first-order sonic and resistivity logs should also show similar character. Nine index samples were obtained within intervals of reliable sonic log. In addition, three core samples, taken at depths of 685.8, 878.1, and 916.6 mbsf (well below the bottom depth of the velocity log), were measured in a velocimeter to compare velocities at atmospheric and in situ pressure (Fig. **F5B**).

The velocities of the core samples were measured in a New England Research velocimeter at in situ differential pressures after the samples were saturated in a fluid of seawater chemistry (Table **T1**). Pore pressures were atmospheric, so confining pressure was equal to differential pressure. Velocimeter accuracy was confirmed by replication of Amoco measurements (Sondergeld and Rai, 1993) on Ferron sandstone samples (Jarrard et al., in press) for both compressional velocity and shear velocity and for both saturated and dry states. These three core plugs were collected during the leg and selected for velocity measurement based on their retention of internal cohesion and cylindrical shape.

A plot of in situ corrected index density vs. in situ corrected index velocity (Fig. **F5C**), for all samples in which both parameters were measured, demonstrates a close relationship between these two porosity-sensitive parameters. We used this relationship to convert logging density values to pseudovelocities. Index density was at no point converted to pseudovelocity as logging densities were. For the portions of the composite velocity curve derived from core data, index velocities were directly used.

The composite velocity and density logs were multiplied together to create the impedance log (Fig. **F6**). The practical effect of using an impedance log rather than just the velocity log is minimal for this site be-

F5. In situ vs. index bulk density and velocity, p. 18.

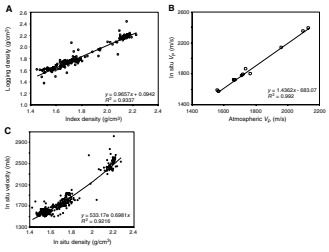

T1. Velocimeter measured in situ pressures, Site 1165, p. 26.

F6. Impedance log and synthetic seismogram, Site 1165, p. 19.

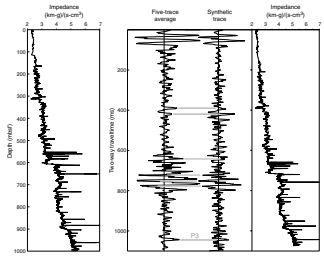

cause the majority of the velocity data are derived from the downhole density log. However, in the nonlogged intervals, some independent character is apparent between density and velocity, although as porosity is the dominant control on both, this is a minor effect.

The resulting synthetic seismogram (Fig. F6) underestimated the depth of the basal reflector by ~7 m in comparison to the original seismic section but matched the depths of the overlying major reflectors. This was corrected by applying a 3% velocity decrease to the pseudovelocity log below 5730 ms. Poor hole conditions may induce velocity shifts of a few percent (e.g., Shipboard Scientific Party, 1989a) through a variety of mechanisms such as borehole wall rebound, wash-outs of loose sediments, or averaging bias across very thin layers or individual cobbles of anomalous velocity.

Site 1166

A reliable *P*-wave velocity log was collected from 367 to 30 mbsf at Site 1166 and forms the main basis of the synthetic seismogram for this site. Since only two index samples were collected from the seafloor to the top of the log, the region of the composite velocity section above the log was based on an assumed seafloor velocity of 1.5 km/s, increasing linearly to 1.9 km/s at a depth of 2.6 mbsf, and then increasing linearly at a rate consistent with the average increase of the logged portion of the same diamict unit (Fig. F7). The change in velocity at 2.6 mbsf is based on observed hemipelagic sediments in the upper 2.6 m of the core, changing to diamict below.

Because of the poor hole conditions at Site 1166, the density log would have required extensive editing. As a result of poor core recovery, index densities were infrequently measured and were probably not representative of overall lithologic variations. Consequently, the composite velocity log was taken as the impedance log (Fig. F7) by assuming a constant density. Since porosity is the dominant control on both velocity and density, using only one as the impedance log is justified here.

Although the velocity log for Site 1166 is generally of good quality, it apparently still contains minor artifacts. After generation of an initial synthetic seismogram for the AGSO line, two spikes, from 114.8 to 120.5 mbsf (0.1087–0.1142 seconds below seafloor [sbsf]) and 304.7 to 309.9 mbsf (0.2722–0.2764 sbsf), were removed from the composite velocity log as well as a short region that produced an anomalous reflection coefficient from 295.1 to 296.2 mbsf (0.263–0.264 sbsf).

Site 742

The Site 742 impedance log was also created from the velocity log only (Fig. F8). We assumed a constant density for essentially the same reasons as for Site 1166. Sonic logging data were collected from ~33 to 270 mbsf, whereas the total depth of Site 742 was 316 mbsf. The lower 46 m of the hole contains 21 index velocity measurements, but they were not included in the impedance log for two reasons. First, these index velocities were anomalously low. All of these index values were measured along the z-axis, which is most sensitive to core disturbance through loss of internal cohesion caused by separation along lithologic planes. Such separation is common in RCB or XCB sections through rotational shearing of semilithified sediments. Second, the sample spacing of index velocities is insufficient to pinpoint impedance contrasts over short intervals. Index values for the region above the log were also

F7. Original and stretched synthetic seismograms, Site 1166, p. 20.

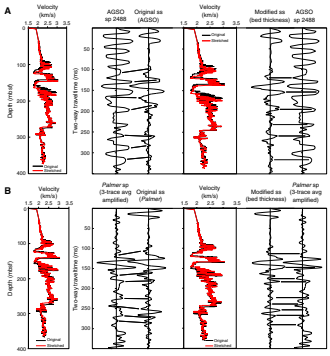

F8. Impedance log and synthetic seismogram, Site 742, p. 21.

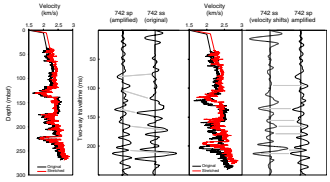

not incorporated into the impedance log, primarily because of low sampling rate. They were used, however, as a guide for the ramping function that bridged the interval from the seafloor to the first log value.

A synthetic seismogram was created for Site 742 during Leg 119 (Shipboard Scientific Party, 1989b). That synthetic seismogram also only used the velocity log as the impedance log, with no use of core samples either above or below. Above the log, a constant velocity of 2.2 km/s was used, which differs from our assumption. We assumed a ramping function that accounts for the ~5.7 m of surficial hemipelagic sediments recovered at the seafloor that overlie the diamict unit that extends beyond the top of the logged interval (Shipboard Scientific Party, 1989b). It is quite possible that the stratigraphic contact between the hemipelagic sediments and the diamict produces a reflector, but not enough data are available to characterize it. Therefore, the ramping function assumes a velocity of 1.5 km/s at the seafloor, linearly increasing to 2 km/s for the top of the diamict. The diamict velocity is then assumed to increase linearly from 2 km/s to the average measured value at the top of the logged section. This produces an extrapolated continuation of the overall trend (Fig. F8).

RESULTS AND DISCUSSION

Site 1165

The synthetic seismogram for Site 1165 (Figs. F6, F9) demonstrates that coring did indeed cross the target reflector, at a depth of ~907 mbsf, in Core 188-1165C-26R. Unfortunately, this core had only 40% recovery. No visible change was seen in any of the cores surrounding the core, either above or below (Fig. F9). Lithostratigraphic Unit III, which composes the lower ~700 m of the section, is generally described as a thinly bedded, fissile claystone (Shipboard Scientific Party, 2001a). More specifically, Core 188-1165C-26R and its neighbors are described as claystone with many silt laminae, typical of contour current–controlled sedimentation on drifts along the Antarctic margin (Stow et al., 2003). The similar internal structure of the cores suggests that bottom-current systems did not change significantly over this interval even though regional seismic geometries (Kuvaas and Leitchenkov, 1992) show that this is the depth at which mounded drift structures begin to develop. X-ray diffraction (XRD) and smear slide analyses indicate a downhole drop in total clay and an increase in silt content at ~900–910 mbsf (Shipboard Scientific Party, 2001b), and this change corresponds with a downhole increase in acoustic impedance that is the source of the reflector. The change in core lithologies across reflector P3 (i.e., same as P2 of Kuvaas and Leitchenkov, 1992) may instead result from sediment source or paleoceanographic variations that accompanied the early construction of the sediment drift features.

An intermediate-depth packet of large reflectors from ~5560 to 5660 ms below the seafloor is centered around the opal-A/opal-CT diagenetic transition (Fig. F9), which was crossed at ~600 mbsf. The width of the reflector packet results from transition thickness and wavelet length; it is initiated by the occurrence of the first chert layer at 492 mbsf and continues through the tail end of propagation through the opal transition (Fig. F9). The opal-A/opal-CT transition increases velocity via porosity decrease, cementation, and improved intergrain contact; it

F9. Synthetic seismogram, lithostratigraphy, and seismic section, Site 1165, p. 22.

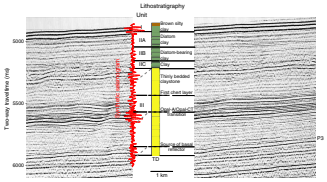

increases bulk density via decreased porosity and increased grain density.

The shallowest regional reflector, at ~5250 ms (~305 mbsf), represents the lithostratigraphic Unit II–III transition from structureless greenish gray clay with dispersed sand grains and lonestones of Unit II to the laminated, fissile, thinly bedded claystone characteristic of Unit III (Fig. F9). This transition has been explained as a mid-Miocene provenance shift (Shipboard Scientific Party, 2001a) and is synchronous with a large drop in mass accumulation rate (Handwerger and Jarrard, 2003).

Site 1166

Two major regional reflectors characterize the seismic section across Site 1166 (Fig. F10). The deeper of these, at ~910 ms (more apparent in the AGSO section), is caused by the Unit III–IV transition. The upper reflector, centered at ~800 ms, occurs in a portion of the core with several large and closely spaced impedance contrasts. As mentioned earlier, one of the primary motivations for creating a synthetic seismogram for this site was to determine how this reflector packet is generated by these adjacent impedance changes. To aid in this characterization, a simplified impedance model was also constructed (Fig. F11) for sensitivity analysis. This model consists of flat-lined average values for each log unit, eliminating the natural but small-scale variability in the data. By using both the real and simplified impedance logs as guides, it was determined that the reflector packet begins at the lithostratigraphic Subunit IB–IC transition and ends with the trailing end of wavelet propagation across the Unit II–III transition (Fig. F10). The sensitivity analysis demonstrates that the large amplitude of the reflectors results from the similar thicknesses of Subunits IC and ID, such that wavelet propagation across the Subunit IB–IC transition and Subunit ID–Unit II transition almost perfectly interfere constructively.

Site 1166 was planned to be drilled on the AGSO line. However, because of ice conditions, it was located ~800 m southwest of the line. In February 2001, the *Palmer* returned to Prydz Bay and recorded a new seismic line that passed ~15 m south of Site 1166 and continued to ~16 m south of Site 742 and beyond (Fig. F1). For both the *Palmer* and AGSO lines, synthetic seismograms adequately mimic the character of the nearest shotpoints to Site 1166 (shotpoint 2488 for the AGSO line and shotpoint 2637 for the *Palmer* line), but two-way traveltimes of major reflectors differ between the seismic and synthetics (Fig. F7). There are two possible causes of the mismatch: changes in bed thicknesses between the drill site and the AGSO seismic line or inaccurate velocities recorded in the sonic log. Traveltime discrepancies are different between the AGSO and *Palmer* lines, so velocity errors alone cannot be the explanation.

Bed thicknesses were adjusted to refine the match of arrival times and shapes of the reflectors to each seismic line. New synthetic seismograms were created from impedance logs that were altered by differentially stretching or compressing the Site 1166 impedance log along identified logging-based unit or subunit boundaries until the best match was obtained (Fig. F7). The amount of stretch and compression needed to match the AGSO shotpoint was different than that needed to match the *Palmer* shotpoint. This further suggests that bed thickness changes are partly responsible for the traveltime mismatches since the starting point for each (the Site 1166 impedance log) was the same. Bed thickness changes are not an unlikely possibility in a fluvio-deltaic sys-

F10. Lithostratigraphy, synthetic seismogram, and impedance log, Site 1166, p. 23.

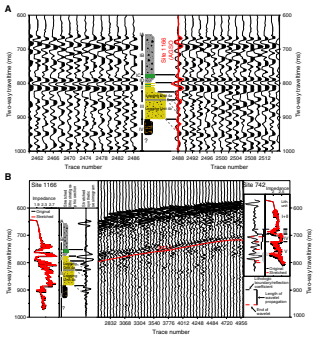

F11. Original and stretched synthetic seismograms based on impedance log, Site 1166, p. 24.

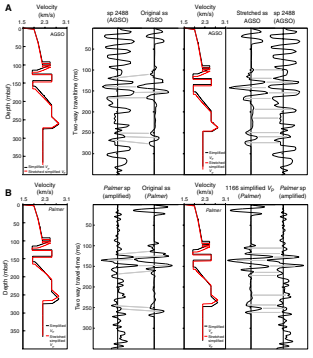

tem, and a laterally variable subsurface geology has been suggested for Site 1166 (**Erohina et al.,** this volume).

A comparison between the original seismic trace and the stretched/compressed trace created to match the AGSO and *Palmer* lines is shown in Figure **F7.** The lithologic boundary changes resulting from this stretching and compression are shown in Table **T2.** Any changes in the thickness of lithostratigraphic Unit IV are not evaluated by the synthetic seismogram because the sonic log did not record any major changes associated with the poorly defined Unit IV/V boundary. It is likely that the impedances of Units IV and V are similar and do not cause a reflector, as both are composed of laminated clays (Shipboard Scientific Party, 2001c). Furthermore, both seismic sections have poor resolution at traveltimes >0.30 sbsf, where the Unit IV/V boundary occurs.

An attempt to match synthetic seismograms to each shotpoint was also undertaken by revising the velocity profile. In each case, different beds required different velocity shifts, with most of the needed velocity changes >5% (more than ~100 m/s) (Fig. **F12**), higher than would be expected (~3%). Cochrane and Cooper (1991) compare sonobuoy data to sonic logging data at Site 742 and suggest that observed differences of ~100 m/s, in regions of complex stratigraphy with thin layers, are "significant," whereas the velocity differences needed to match the synthetic seismogram to the seismic profiles in our study are greater than this. We conclude that bed thickness changes are more likely than these large velocity shifts (Table **T3**) to be the dominant control on reflector mismatches.

One discrepancy between lithostratigraphic and log-based units is the existence of logging subunits (4a and 4b) within the single lithostratigraphic Unit III (Fig. **F10**). Subunit 4a is a transition zone, with logging values oscillating between those typical of underlying Subunit 4b and overlying Unit 3 (lithostratigraphic Unit II) (Fig. **F10B**). Lithostratigraphic Unit III averaged only ~14% recovery, predominantly loose sands, and was therefore unable to detect this transitional character. The best fit between the synthetic seismograms for Site 1166 and each of the seismic lines requires that the two log-defined subunits be distinct and differentially stretched or compressed relative to each other. Treating the two subunits as only a single major unit does not produce as close a match.

The most significant Cenozoic event in Prydz Bay is the transition from preglacial to full-glacial paleoenvironments. The transition occurs at Site 1166 between Late Cretaceous and early Pliocene time within lithostratigraphic Units IV, III, II, and I (Shipboard Scientific Party, 2001c; Cooper et al., 2001; **Cooper and O'Brien,** this volume). Within the early glacial massive sands of Unit III, sand grain surface textures indicate an uphole-increasing component of glaciers in hinterland mountains (Strand et al., 2003). The upper part of Unit III, corresponding to the transitional logging Subunit 4a, denotes a time when Site 1166 had nearby cool-climate vegetation and was near sea level in a fluvio-tidal depositional setting and accumlating outwash sands and clays (**Macphail and Truswell,** this volume). The boundary between the lower part of Unit III (massive sands) and upper part of Unit III (alternating sands and silts) is clearly visible in downhole logs and it produces a reflection in the synthetic seismic trace (Fig. **F10**). But the boundary does not produce a single significant seismic reflector of regional extent (**Erohina et al.,** this volume; Fig. **F10**). The lithologic sand/silt variations may instead be a feature of the fluvio-tidal deposits

T2. Bed thickness changes applied to impedance logs, Sites 1166 and 742, p. 27.

F12. Velocity modification of impedance logs, Site 1166, p. 25.

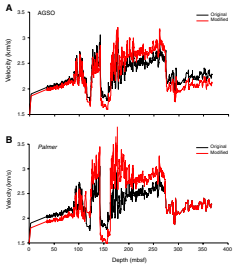

T3. Velocity changes applied to impedance logs, Sites 1166 and 742, p. 28.

near Site 1166. In support of this, **Erohina et al.** (this volume; Fig. **F3**) show that Unit III at Site 1166 either lies at the bottom of or below the section drilled at Site 742. The drill cores show that the upper two-thirds of lithostratigraphic Unit III does not have a counterpart at Site 742 (Shipboard Scientific Party, 2001c), and no preglacial rocks were recovered at Site 742 (Shipboard Scientific Party, 1989b).

Site 742

The upper part of Site 742 is similar to the upper portion of Site 1166, as illustrated by the similarity of the impedance logs (Fig. **F10B**). The Subunit ID–Unit II transition at Site 1166 correlates with the Unit IV–V transition at Site 742. The same reflector packet that starts at Subunit IC at Site 1166 starts with the top of Unit III at Site 742. As the Unit IV–V transition at Site 742 is the last contributor to the reflector packet, it marks the base of acoustic unit PS.1 (Fig. **F10B**), as defined by Cooper et al. (1991) and Cochrane and Cooper (1991). It can be traced along the *Palmer* line between the sites.

A reflector in the synthetic seismogram that corresponds to a thin bed at ~225 mbsf (Fig. **F8**) is likely a local effect. The bed itself was not recovered in the core, but its appearance in most of the logs confirms that it is not an artifact of the acoustic log. The reflection at this depth can be traced ~18 km southwest from the drill site along the *Palmer* line (**Erohina et al.,** this volume; Fig. **F3**). The heterogeneous acoustic signature of the underlying interval, which is composed of waterlain tills, suggests variability, but this unit can be traced in the *Palmer* data to within a kilometer of Site 1166, where it is too thin to be resolved (**Erohina et al.,** this volume; Fig. **F4**).

As with Site 1166, initial comparison of the synthetic seismogram and the shotpoint closest to Site 742 showed a slight mismatch between major reflectors in the synthetic and seismic sections. Refinements were attempted based on adjusting bed thicknesses and bed velocities, similar to the procedure for Site 1166 (Fig. **F8;** Table **T2**). The results suggest subtler shifts than those at Site 1166, which would be expected based on the flatter bedding at Site 742 atop the Four Ladies Bank, in contrast to the location of Site 1166 on the flank of a channel system. In fact, if only the upper unit is assumed to be ~6 m (5%) thinner at the nearest shotpoint on the *Palmer* line than at Site 742 ~16 m away, the synthetic and seismic traces align. In comparison, a 5% increase in velocity of all units except Unit IV, and a 3% velocity reduction there, would also align the synthetic and seismic traces, and this is the assumption we make. The 5% velocity increase is the same for each of the diamict units, whereas the lone nondiamict unit (Unit IV) requires the lesser shift. Furthermore, a 5% correction is reasonable for diamict sediments, due to their loosely packed and often heterogeneous nature.

Sonobuoy studies (Cochrane and Cooper, 1991) as well as the synthetic seismogram (Cooper et al., 1991; Shipboard Scientific Party, 1989b) at Site 742 indicate that both of the above are possibilities. Cochrane and Cooper (1991), for example, observed a mismatch between their sonobuoy velocities and the downhole sonic velocities at Site 742 of up to 0.1 km/s using a top-down ray-trace model. They suggest that this difference may be attributable to both stratigraphic differences between the sonobuoy and drill site positions and an inability of the sonobuoy data to resolve thin beds <10 m thick, which can be detected in the downhole sonic log.

CONCLUSIONS

Synthetic seismograms were generated from logging- and core-based physical properties data for Sites 1165 and 1166 from Leg 188 and Site 742 from Leg 119, in Prydz Bay, Antarctica. The synthetic seismograms allow for the accurate interpretation of the overall seismic section by tying observed recovered lithologies to reflectors in the seismic profiles. These results provide a foundation for seismic-based regional lithologic and facies interpretation in Prydz Bay (**Erohina et al.,** this volume)

The synthetic seismogram for Site 1165 demonstrates that target reflector P3 was penetrated by drilling. Core lithologies change across this reflector, and these changes may result from sediment-source or paleoceanographic variations that accompanied the early construction of the sediment drift features. Other reflectors identified at the site correspond to the opal-A/opal-CT diagenetic transition and to an interval of decelerating mass accumulation rate.

The seismic stratigraphies of Sites 1166 and 742 are dominated by a series of closely spaced reflectors at ~0.15 sbsf. This reflector set is created by a suite of prominent, closely spaced impedance contrasts and can be traced between the sites. Similar lithologies are seen at both sites within acoustic unit PS.1, identified by Cooper et al. (1991). Below this, however, Site 742 contains a succession of glaciomarine diamictites, minor sands, and siltstones, whereas Site 1166 has marine claystone (diamictite) sands and clays and massive sands. At Site 742, the diamictite sediments below PS.1 lie within acoustic unit PS.2A1. This acoustic unit can be traced across the *Palmer* line to within a kilometer of Site 1166, (**Erohina et al.,** this volume; Fig. **F3**). At both sites, adjustments to the impedance logs, either through bed thickness changes or velocity changes, were needed to synchronize the reflectors in the synthetic seismograms with the reflectors in the seismic sections. The adjustment was greater for Site 1166 than for Site 742, with more adjustment of Site 1166 relative to the AGSO line than for the *Palmer* line. This likely results from the fact that Site 1166 was drilled ~800 m off the AGSO line, while the *Palmer* line passed within 30 m of the site. Furthermore, Site 1166 was drilled on the flank of a fluvio-deltaic channel system, whereas Site 742 was drilled in a more geologically uniform, prograding sequence.

ACKNOWLEDGMENTS

This research used data and samples provided by the Ocean Drilling Program (ODP). ODP is sponsored by the U.S. National Science Foundation (NSF) and participating countries under management of Joint Oceanographic Institutions, Inc. (JOI). This project was funded, in part, by grant 188-F001224 from the U.S. Science Support Program to D.A. Handwerger.

REFERENCES

Cochrane, G.R., and Cooper, A.K., 1991. Sonobuoy seismic studies at ODP drill sites in Prydz Bay, Antarctica. *In* Barron, J., Larsen, B., et al., *Proc. ODP, Sci. Results,* 119: College Station, TX (Ocean Drilling Program), 27–44.

Cooper, A., Stagg, H., and Geist, E., 1991. Seismic stratigraphy and structure of Prydz Bay, Antarctica: implications from Leg 119 drilling. *In* Barron, J., Larsen, B., et al., *Proc. ODP, Sci. Results,* 119: College Station, TX (Ocean Drilling Program), 5–26.

Cooper, A.K., O'Brien, P.E., and ODP Leg 188 Shipboard Scientific Party, 2001. Early stages of east Antarctic glaciation—insights from drilling and seismic reflection data in the Prydz Bay region. *In* Florindo, F., and Cooper, A.K. (Eds.), *The Geologic Record of the Antarctic Ice Sheet from Drilling, Coring and Seismic Studies*. Quad. Geofis., Inst. Naz. Geofis. Vulcanol., 16:41–42. (Abstract)

Hamilton, E.L., 1976. Variations of density and porosity with depth in deep-sea sediments. *J. Sediment. Petrol.,* 46:280–300.

————, 1979. Sound velocity gradients in marine sediments. *J. Acoust. Soc. Am.,* 65:909–922.

Handwerger, D.A., and Jarrard, R.D., 2003. Neogene changes in Southern Ocean sedimentation based on mass accumulation rates at four continental margins. *Paleoceanography,* 18(4):1081. DOI 10.1029/2002PA000850.

Jarrard, R.D., Sondergeld, C.H., Chan, M.A., and Erickson, S.N., in press. Petrophysics of the Ferron Sandstone, central Utah. *In* Chidsey, T.C. (Ed.), *The Fluvial-Deltaic Ferron Sandstone: Regional to Wellbore Scale Outcrop Analog Studies and Application to Reservoir Modeling*. AAPG Mem.

Kuvaas, B., and Leitchenkov, G., 1992. Glaciomarine turbidite and current-controlled deposits in Prydz Bay, Antarctica. *Mar. Geol.,* 108:365–381.

Shipboard Scientific Party, 1989a. Site 721. *In* Prell, W.L., Niitsuma, N., et al., *Proc. ODP, Init. Repts.,* 117: College Station, TX (Ocean Drilling Program), 197–254.

————, 1989b. Site 742. *In* Barron, J., Larsen, B., et al., *Proc. ODP, Init. Repts.,* 119: College Station, TX (Ocean Drilling Program), 397–458.

————, 2001a. Leg 188 summary: Prydz Bay–Cooperation Sea, Antarctica. *In* O'Brien, P.E., Cooper, A.K., Richter, C., et al., *Proc. ODP, Init. Repts.,* 188, 1–65 [CD-ROM]. Available from: Ocean Drilling Program, Texas A&M University, College Station TX 77845-9547, USA.

————, 2001b. Site 1165. *In* O'Brien, P.E., Cooper, A.K., Richter, C., et al., *Proc. ODP, Init. Repts.,* 188, 1–191 [CD-ROM]. Available from: Ocean Drilling Program, Texas A&M University, College Station TX 77845-9547, USA.

————, 2001c. Site 1166. *In* O'Brien, P.E., Cooper, A.K., Richter, C., et al., *Proc. ODP, Init. Repts.,* 188, 1–110 [CD-ROM]. Available from: Ocean Drilling Program, Texas A&M University, College Station TX 77845-9547, USA.

Sondergeld, C.H., and Rai, C.S., 1993. A new exploration tool: quantitative core characterization. *Pure Appl. Geophys.,* 141:249–268.

Stow, D.A.V., Pudsey, C.J., Howe, J.A., Faugeres, J.-C., and Viana, A.R. (Eds.), 2003. *Deep-Water Contourite Systems: Modern Drifts and Ancient Series, Seismic and Sedimentary Characteristics.* Mem.—Geol. Soc. (London, U.K.).

Strand, K., Passchier, S., and Näsi, J., 2003. Implications of quartz grain microtextures for onset of Eocene/Oligocene glaciation in Prydz Bay, ODP Site 1166, Antarctica. *Palaeogogr., Palaeoclimatol., Palaeoecol.,* 198:101–111.

Figure F1. Location map for ODP sites and AGSO and *Palmer* seismic lines.

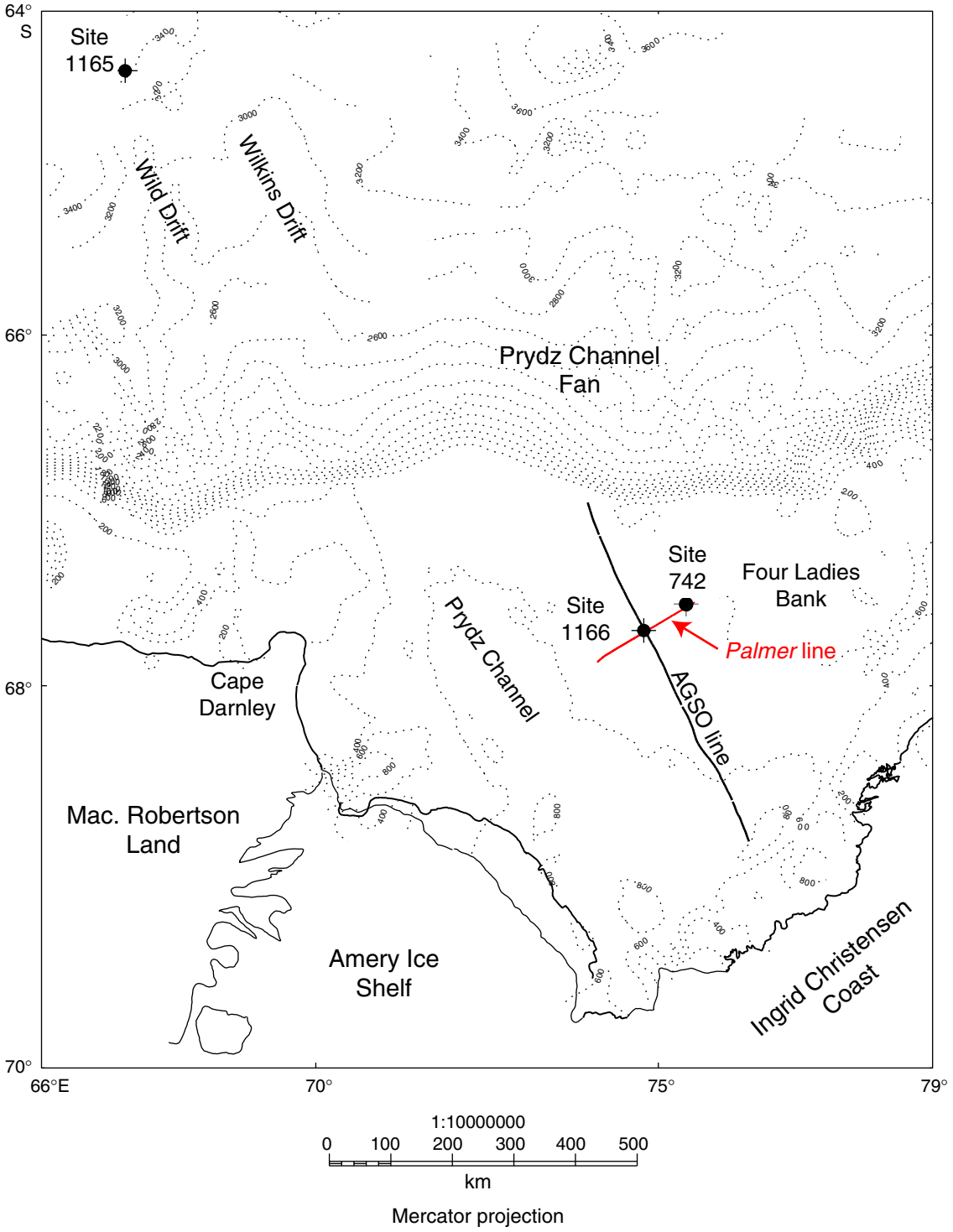

Figure F2. Seismic section for Site 1165 showing regional reflectors and position of drill hole. Adapted from Shipboard Scientific Party (2001b).

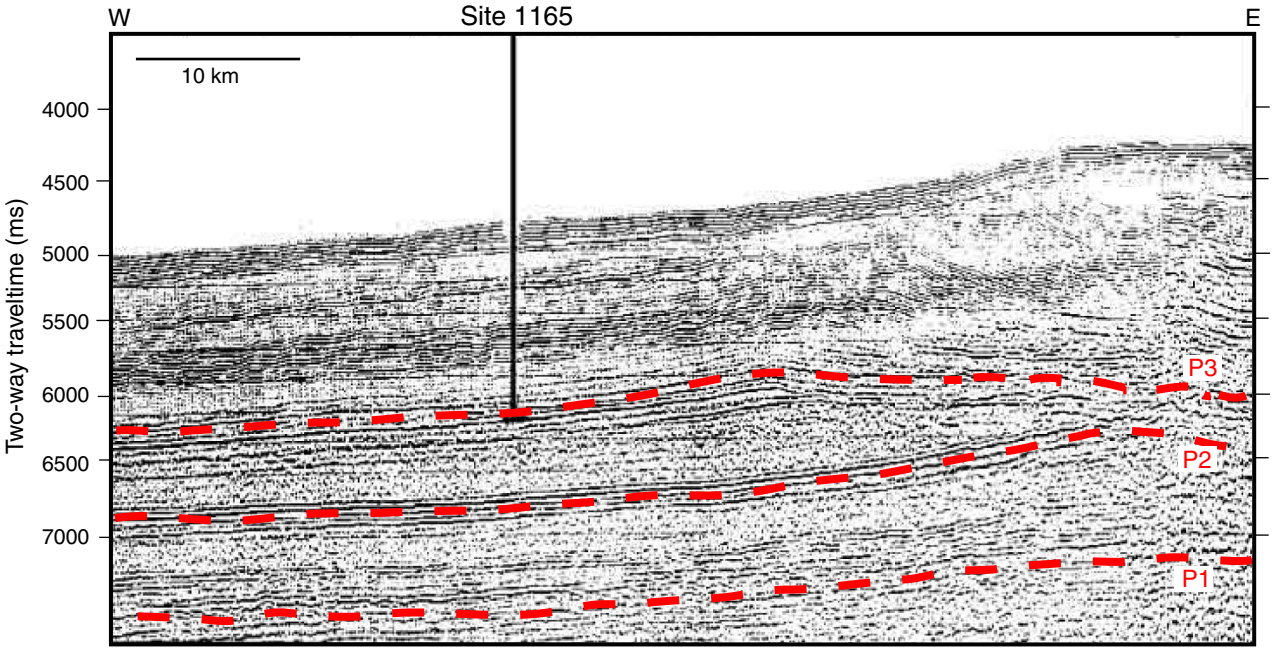

Figure F3. A. AGSO seismic section for Site 1166. The drill site actually lies ~780 m southwest of the line. **B.** *Palmer* seismic section for Sites 1166 and 742. Both drill sites lie within 20 m northwest of the line.

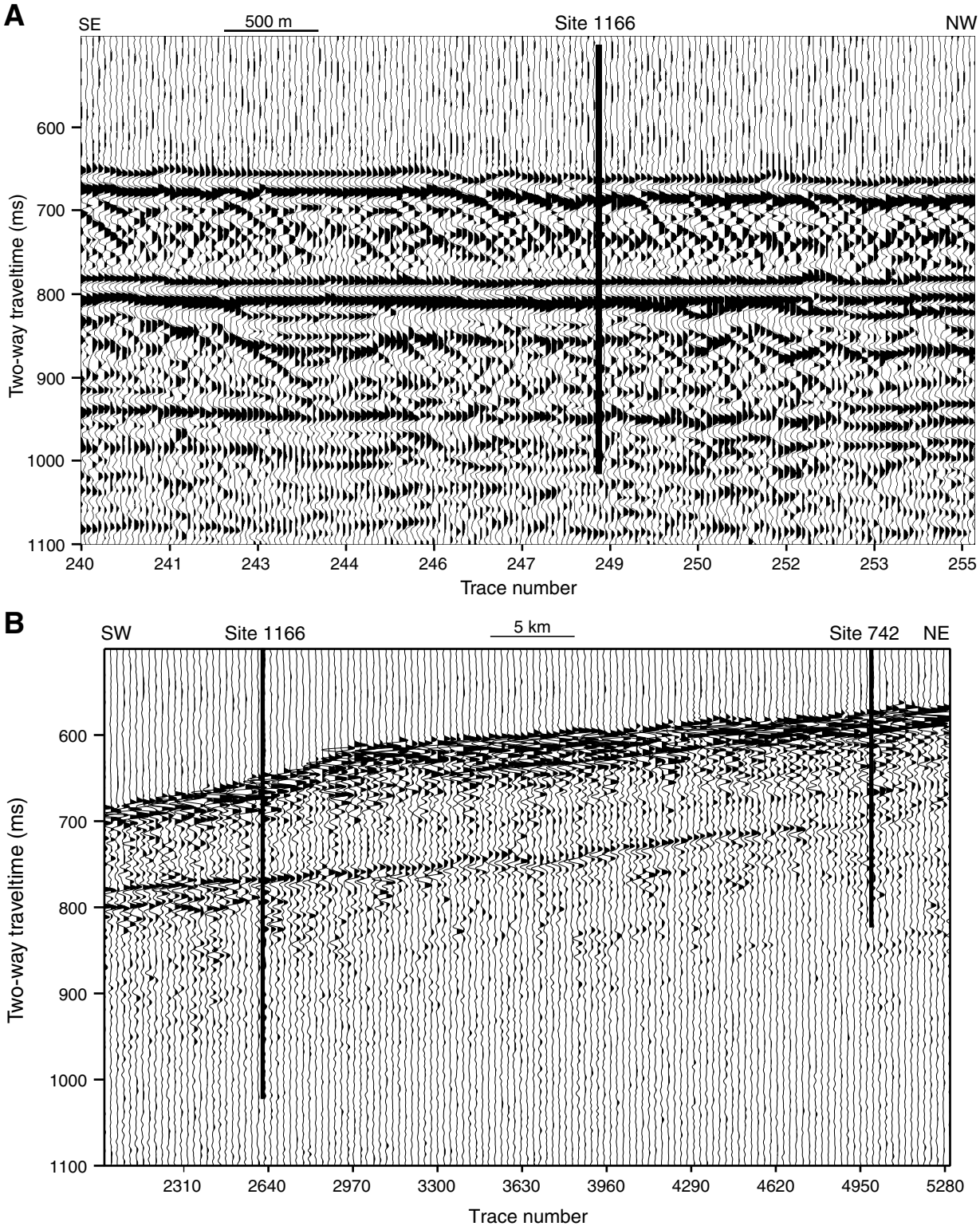

Figure F4. Wavelets used for creating the synthetic seismograms for each seismic profile. **A.** Site 1165 wavelet is based on the average of two widely spaced traces. **B.** AGSO line wavelet is based on the seafloor reflection from trace 1102. **C.** Palmer line wavelet is based on the average of three adjacent traces ~9.5 km southwest of Site 1166. sp = shotpoint.

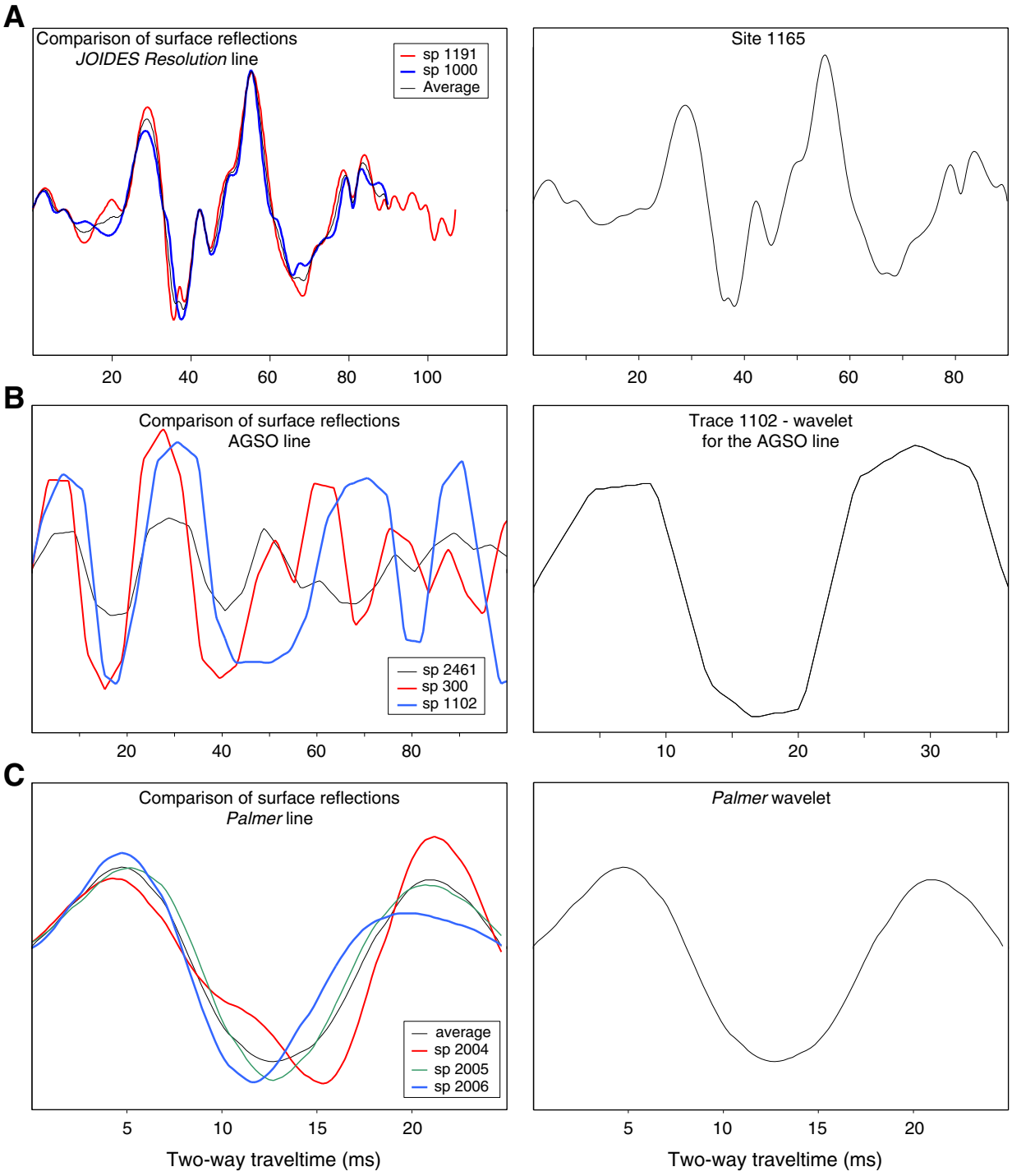

Figure F5. A. Comparison of the logging (i.e., in situ) and index bulk density. Each logging value is the value at the nearest depth to the depth of an index value. **B.** Comparison of in situ *P*-wave velocity and atmospheric pressure *P*-wave velocity. **C.** Comparison of in situ velocity and in situ bulk density (relationship leading to the creation of the pseudovelocity log from the density log).

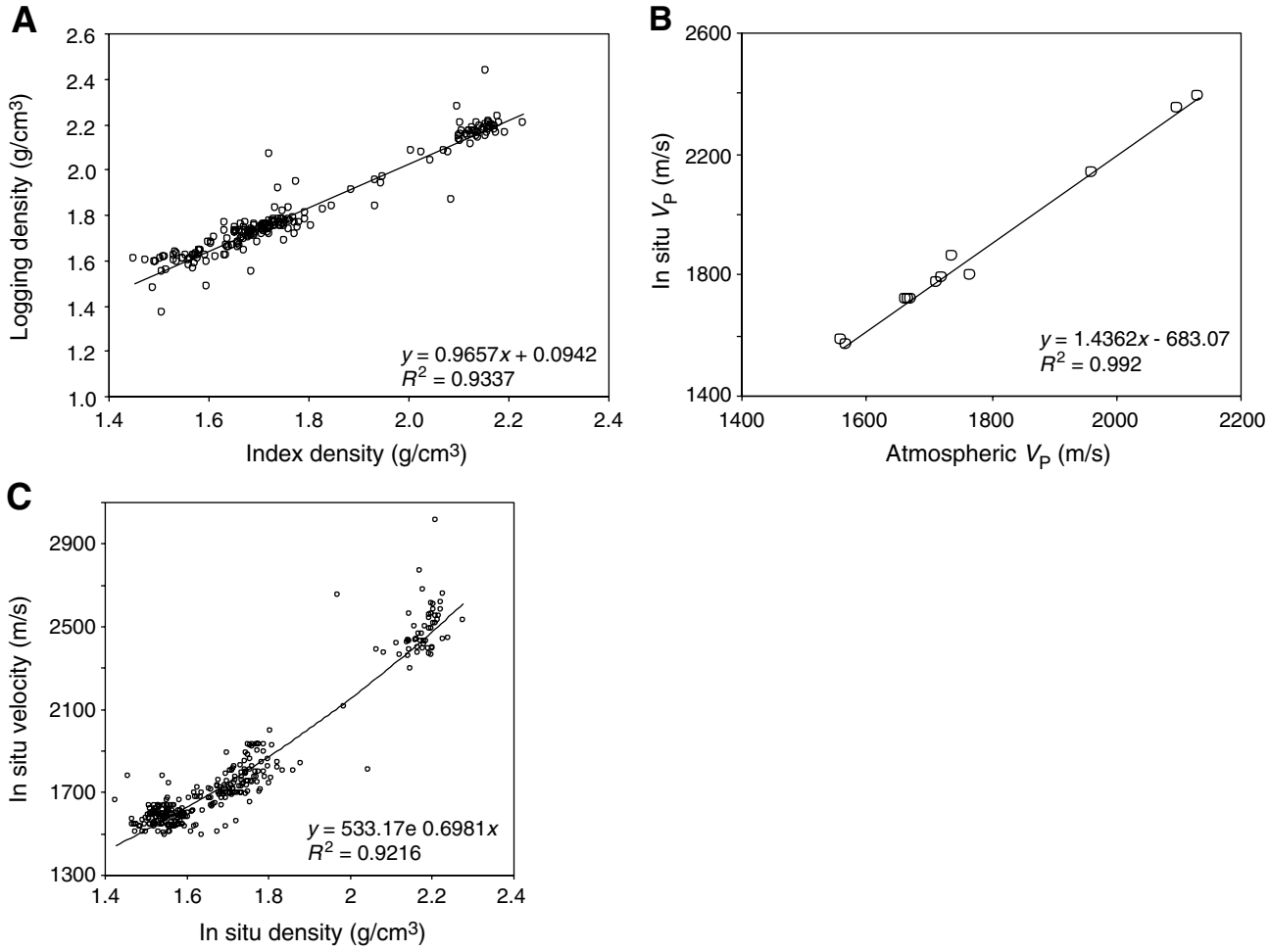

Figure F6. Impedance log and synthetic seismogram for Site 1165 compared to a five trace average about the shotpoint closest to the drill site.

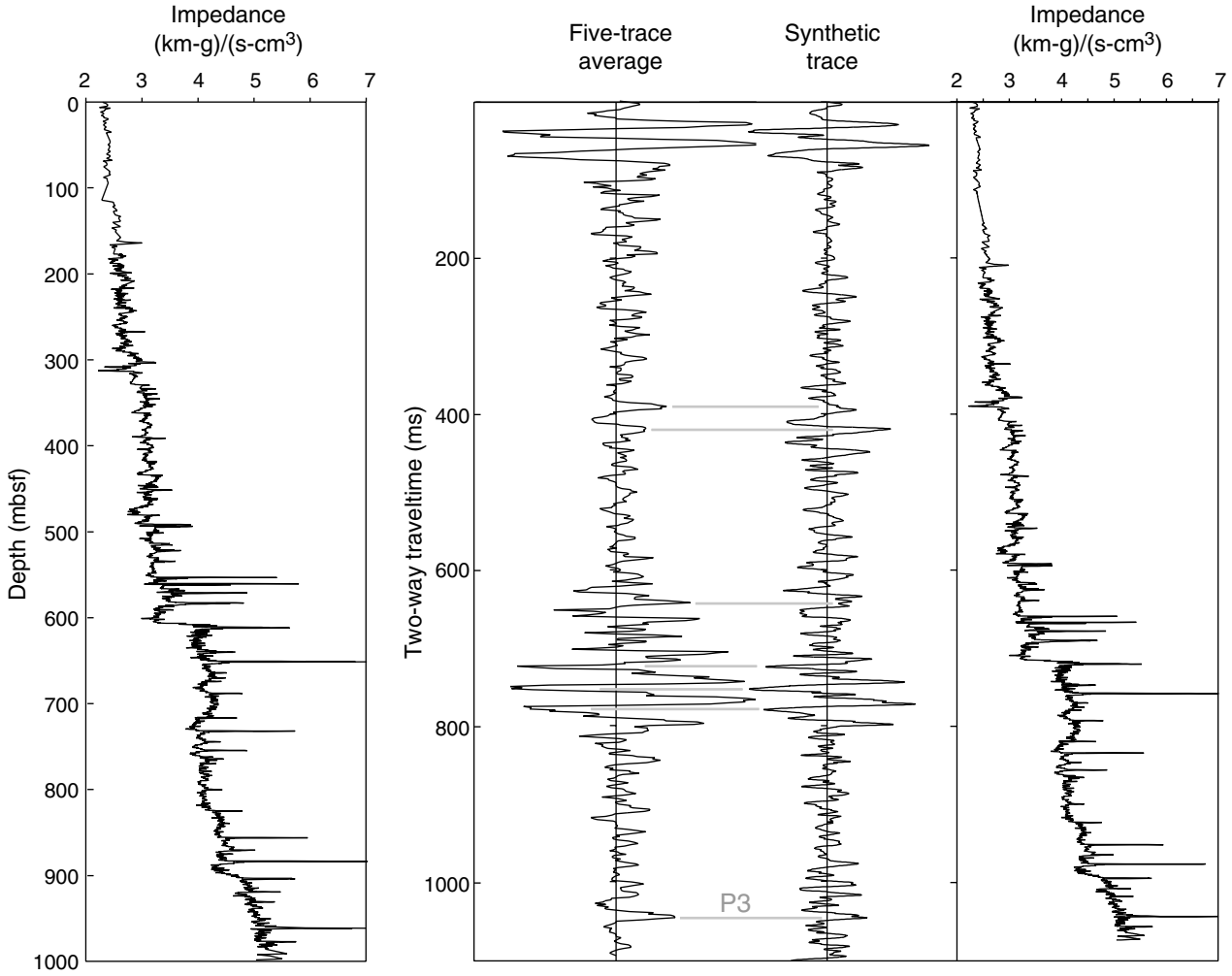

Figure F7. Comparison of original and stretched synthetic seismograms (ss) for both the (A) AGSO and (B) *Palmer* lines and the impedance logs from which they were derived at Site 1166. The *Palmer* shotpoint (sp) trace was amplified by multiplying the original amplitude by (depth)$^{1.5}$. The "original" impedance logs come directly from the logging data while the "stretched" impedance logs are modified versions of the original, designed to produce a synthetic seismogram that directly aligns with the seismic trace.

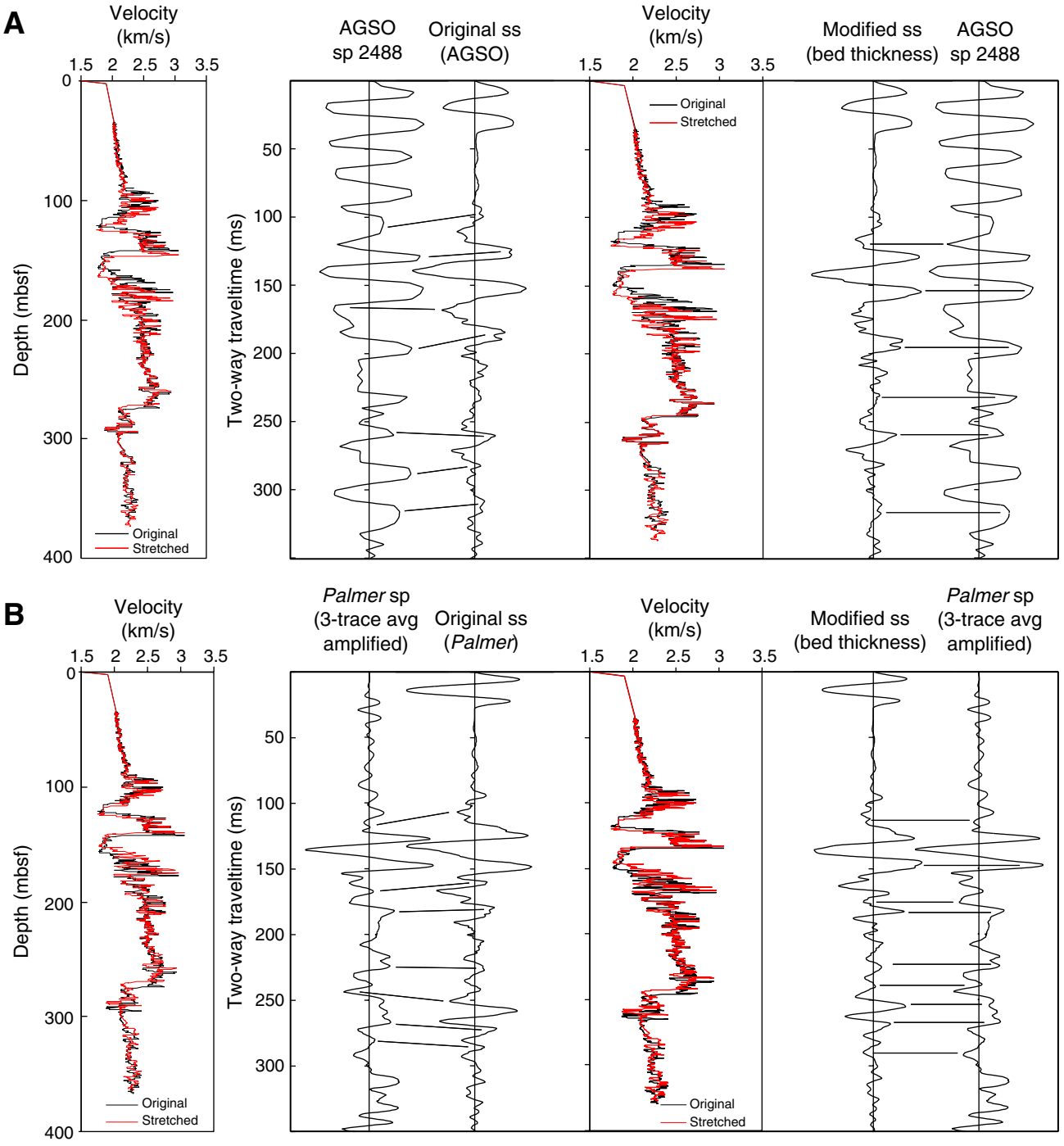

Figure F8. Impedance log and synthetic seismogram (ss) for Site 742 compared to the shotpoint (sp) closest to the drill site on the *Palmer* line. The shotpoint trace was amplified by multiplying the original amplitude by (depth)$^{1.5}$. The "original" impedance log comes directly from the logging data while the "stretched" impedance log is a modified version of the original, designed to produce a synthetic seismogram that directly aligns with the seismic trace.

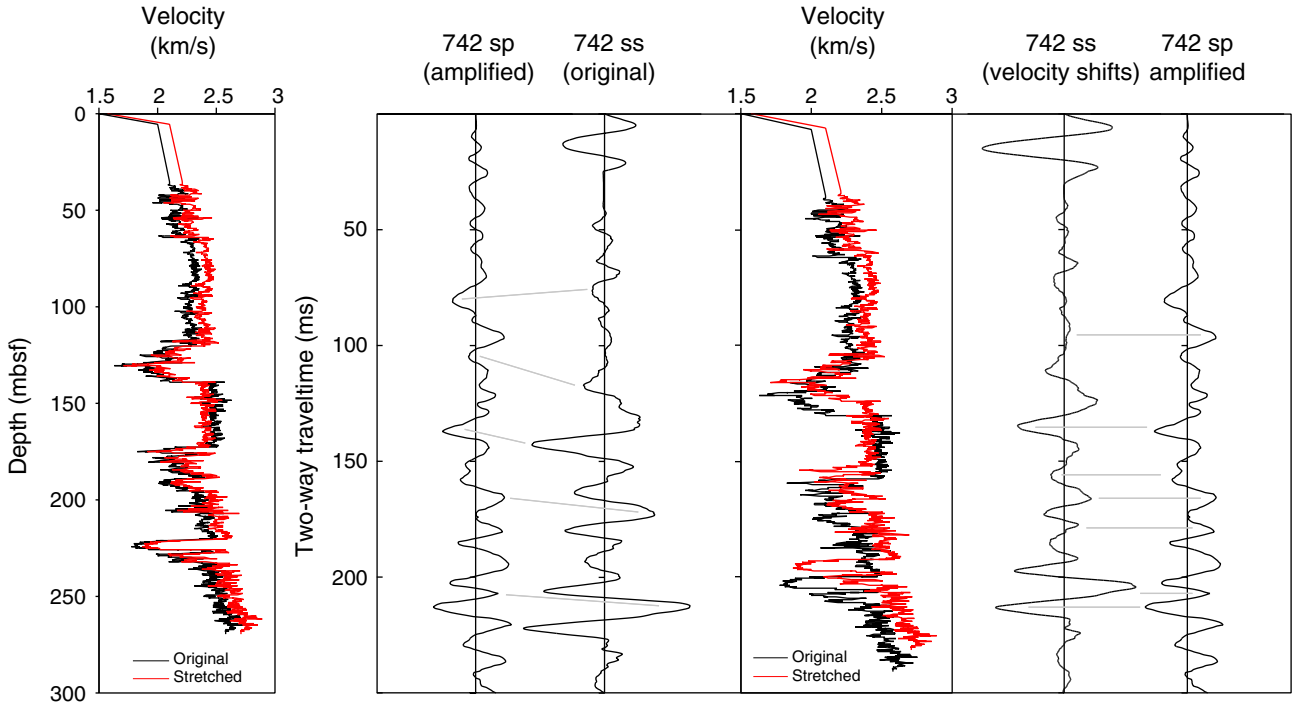

Figure F9. Synthetic seismogram, lithostratigraphy, and shipboard-generated seismic section for Site 1165. Dashed lines represent the end of source wavelet propagation across a given boundary. Seismic section and lithostratigraphic display adapted from Shipboard Scientific Party (2001a).

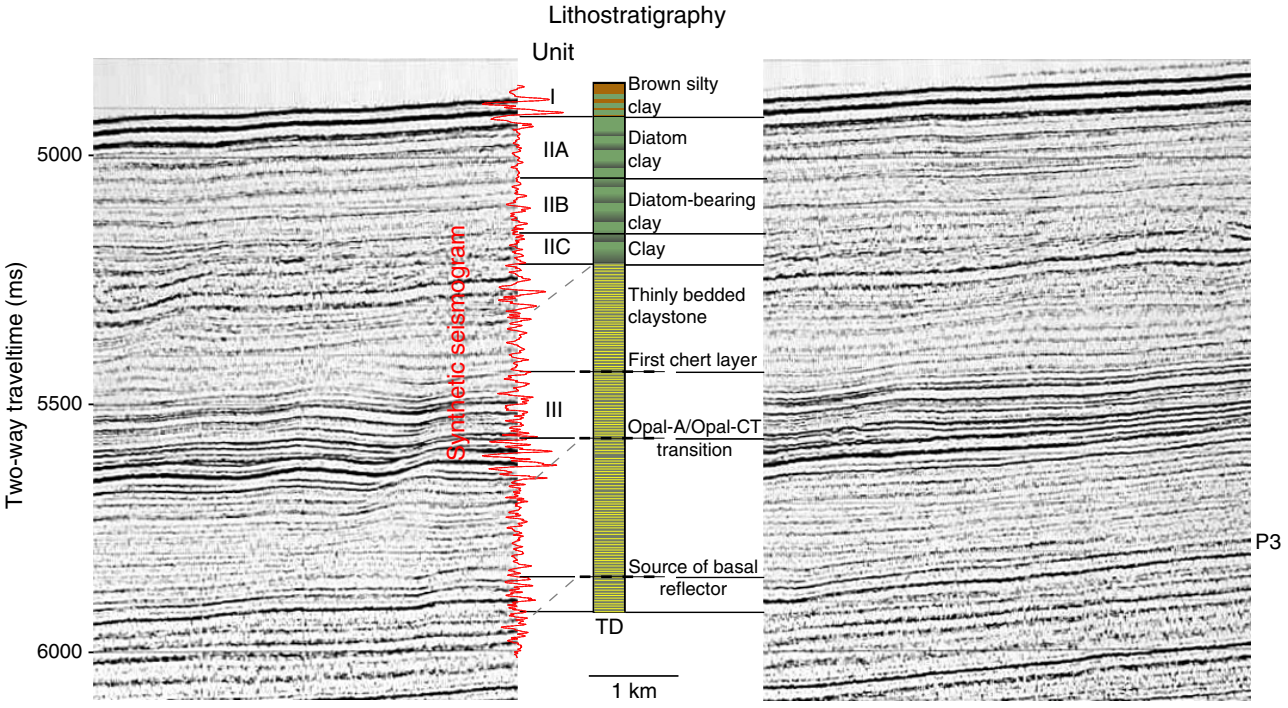

Figure F10. A. Lithostratigraphic section for Site 1166 plotted alongside the synthetic seismogram for the AGSO line. **B.** Lithostratigraphic section and impedance log for Site 1166 and the impedance log for Site 742, each plotted with their respective synthetic seismograms alongside the nearest shotpoints on the Palmer line to the drill sites. The solid lines extending from the Site 1166 lithostratigraphic section to the synthetic traces on each plot represent the onset of wavelet propagation at an impedance contrast. Gray dashed lines reflect the trailing edge of wavelet propagation. The equivalent markings for Site 742 are shown in the key below the Site 742 synthetic seismogram.

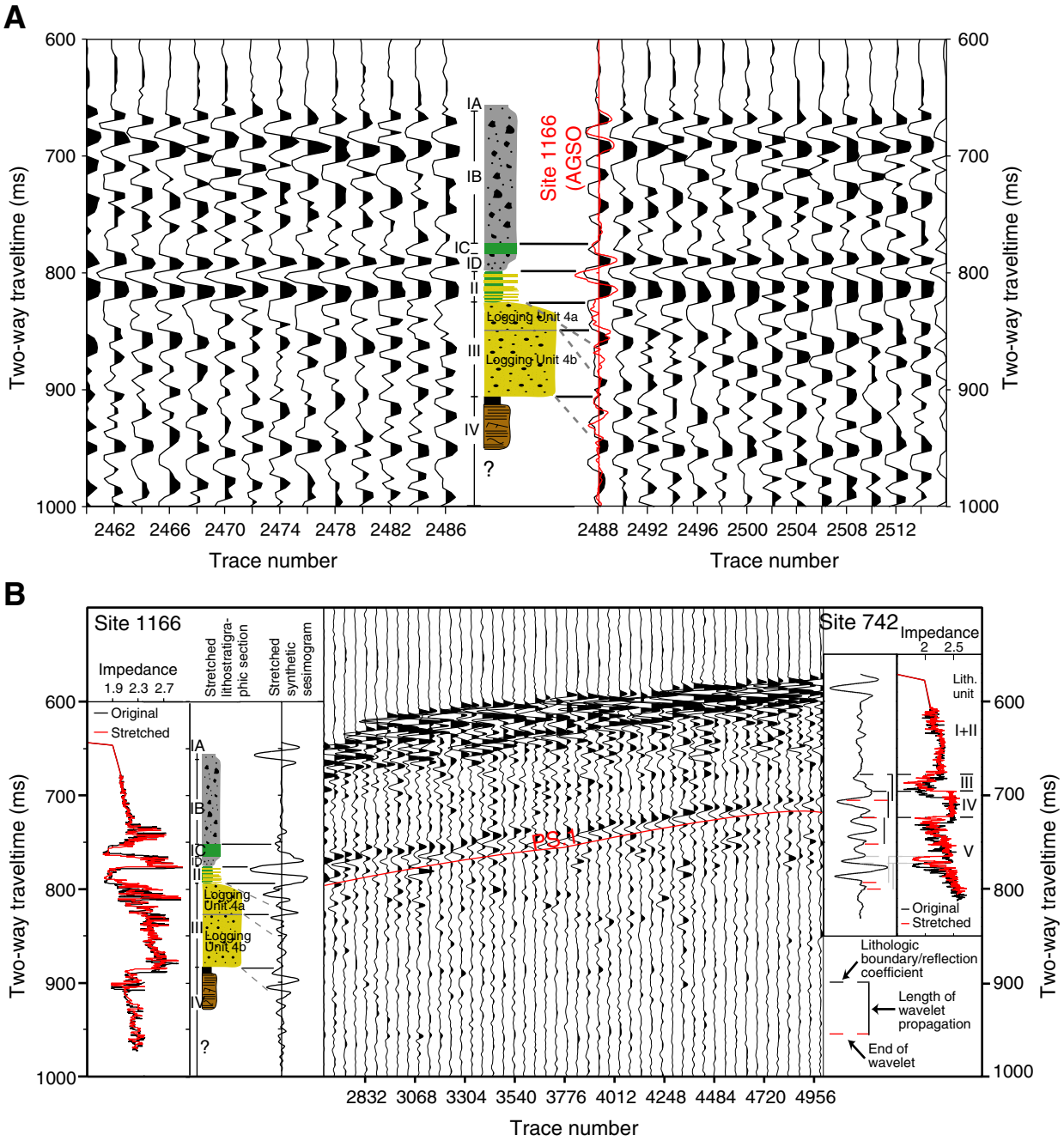

Figure F11. Comparison of original and stretched synthetic seismograms (ss) based on modeled simplification of the Site 1166 impedance log for both the (**A**) AGSO and (**B**) *Palmer* lines. The stretching factors are the same as for the original impedance logs.

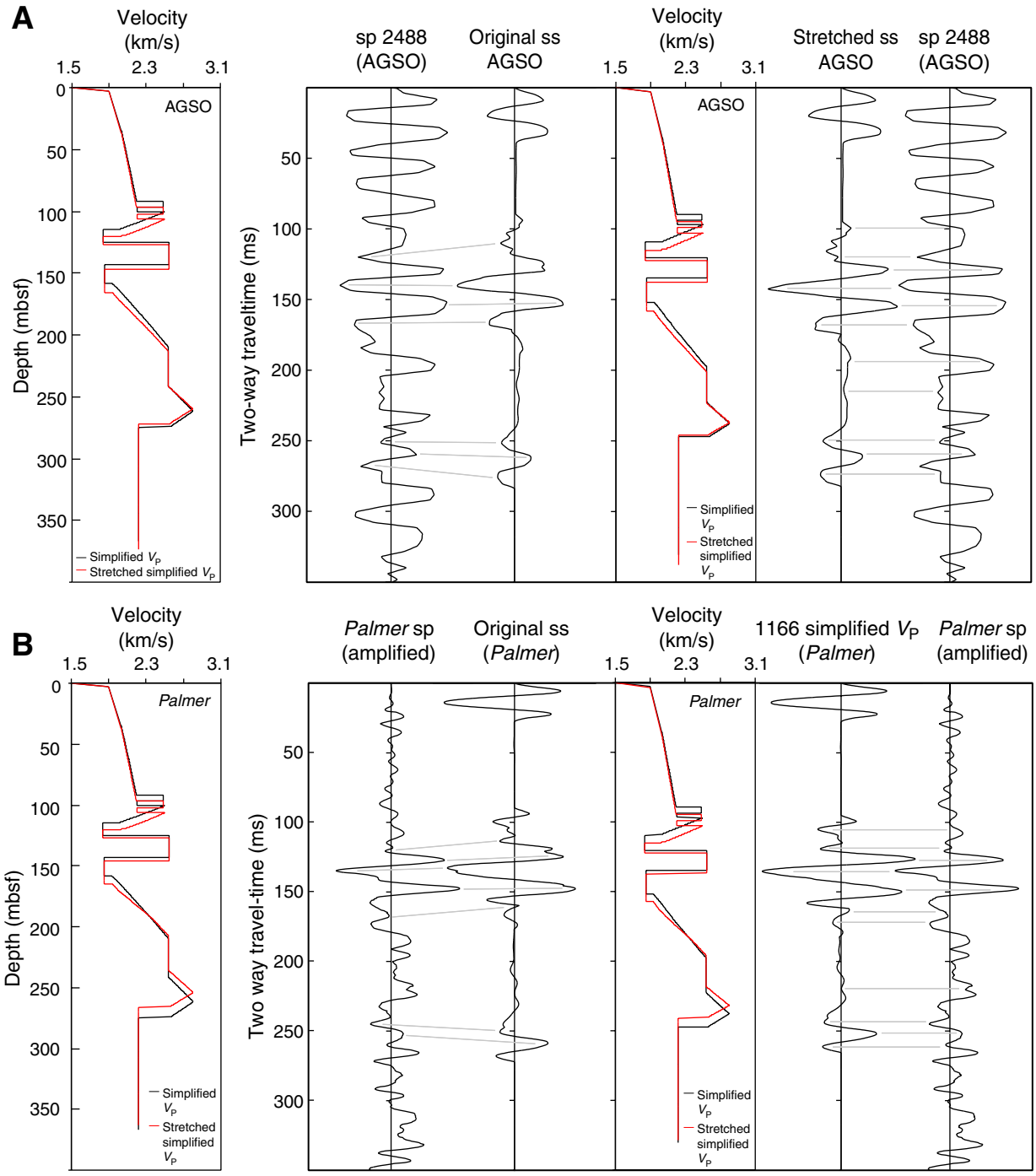

Figure F12. Velocity modification of the original impedance logs for Site 1166 needed to match the synthetic seismograms to the nearest shotpoint on the (**A**) AGSO line and (**B**) *Palmer* line. The needed shifts are larger than would be expected and are therefore unrealistic. sp = shotpoint.

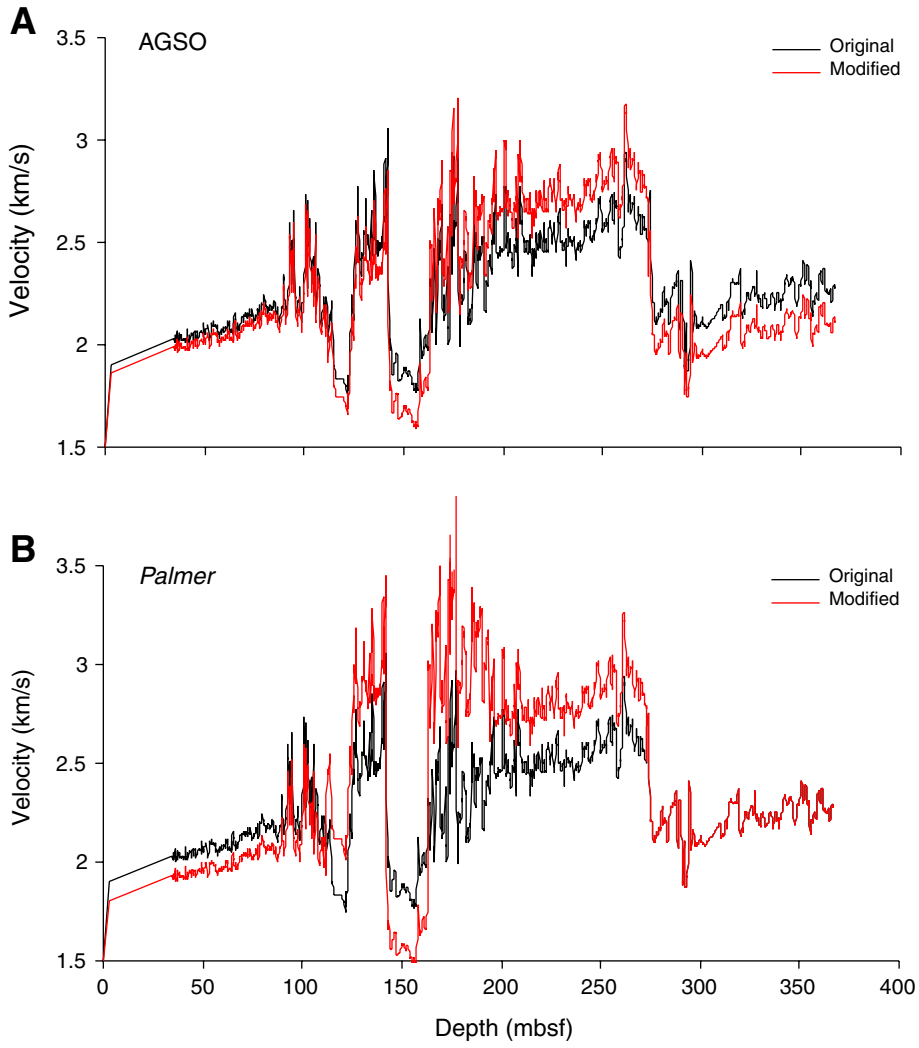

Table T1. Velocimeter measured in-situ pressures of Site 1165 core samples.

Sample depth (mbsf)	Index V_P (m/s)	Atmospheric V_P (m/s)	150 psi V_P (m/s)	In situ V_P (m/s)	In situ/ atmospheric	In situ/ 150 psi	In situ/ index
685.8	1907.5	1965	2018	2132	1.085	1.056	1.118
878.1	2103	2135	2248	2383	1.116	1.06	1.133
916.6	2250	2100	2163	2350	1.119	1.086	1.044

Note: Index V_P (*P*-wave velocity) was measured shipboard during the cruise, differential, atmospheric, and in situ V_P were measured in the velocimeter.

Table T2. Bed thickness changes applied to the Sites 1166 and 742 impedance logs to match the synthetic seismograms to the seismic profiles.

Lithostratigraphic unit	Logging unit	Lower boundary (mbsf)	Modified lower boundary (mbsf)	Unit thickness (m)	Modified unit thickness (m)	Thickness change (m)	Thickness change (%)
Palmer line (Site 1166)							
IB	2a	112.1	114.3	112.1	114.3	2.2	2
IC	2b	125	127.2	13	12.9	0	–0.3
ID	2c	142.1	140	17.1	12.8	–4.3	–25
II	3	163.1	156.9	21	16.9	–4.1	–19.6
III	4a	194.1	197.1	30.9	40.2	9.2	29.8
III	4b	273	268.2	78.9	71.1	–7.9	–10
IV–V (TD)	5 (TD)	366.9	363.9	93.9	95.8	1.9	2
AGSO line (Site 1166)							
IB	2a	112.1	118.7	112.1	118.7	6.7	5.9
IC	2b	125	127.2	13	8.5	–4.5	–34.5
ID	2c	142.1	146	17.1	18.8	1.7	10.1
II	3	163.1	171.2	21	25.2	4.2	19.8
III	4a	194.1	199.1	30.9	27.8	–3.1	–10
III	4b	273	270.1	78.9	71.1	–7.9	–10
IV–V (TD)	5 (TD)	366.9	373.4	93.9	103.3	9.4	10
Palmer line (Site 742)							
I + II		120.4	110.8	120.4	110.8	9.6	8
III		139	129.4	18.6	18.6	0	0
IV		172.7	179.9	33.7	50.5	–16.8	–50
IV (TD)		269.9	272.3	97.2	92.4	4.9	5

Note: TD = total depth.

Table T3. Velocity changes applied to the Site 1166 and 742 impedance logs to match the synthetic seismograms directly to the seismic profiles.

Lithostratigraphic unit	Logging unit	Lower boundary (mbsf)	Two-way traveltime to base of unit (s)	Modified two-way traveltime to base of unit (s)	Change in original velocity (fraction)
AGSO line (Site 1166)					
IB	2a	112.07	0.1076	0.1098	0.98
IC	2b	125.03	0.121	0.1239	0.95
ID	2c	142.1	0.1344	0.138	0.95
II	3	163.13	0.1565	0.1625	0.9
III	4a	194.07	0.183	0.1871	1.08
III	4b	273.01	0.245	0.2445	1.08
IV–V (TD)	5 (TD)	366.89	0.3297	0.3355	0.93
Palmer line (Site 1166)					
IB	2a	112.07	0.1076	0.1132	0.95
IC	2b	125.03	0.121	0.1248	1.15
ID	2c	142.1	0.1344	0.1365	1.15
II	3	163.13	0.1565	0.1627	0.84
III	4a	194.07	0.183	0.1831	1.3
III	4b	273.01	0.245	0.239	1.11
IV–V (TD)	5 (TD)	366.89	0.3297	0.3237	1
Palmer line (Site 742)					
I + II		120.4	0.1115	0.1062	1.05
III		138.99	0.1301	0.1239	1.05
IV		172.67	0.1573	0.1519	0.97
V (TD)		269.9	0.2409	0.2315	1.05

Notes: TD = total depth. For Site 1166, these changes are too large to be realistic.